N84-32316

CORNELL UNIVERSITY
Center for Radiophysics and Space Research

ITHACA, N. Y.

SEMI-ANNUAL STATUS REPORT

to the

NATIONAL AERONAUTICS AND SPACE ADMINISTRATION

under

NASA Grant NAGW-543

ASTEROID LIGHTCURVE INVERSION

February 15, 1984 - August 15, 1984

Principal Investigator: Professor Steven J. Ostro

CENTER FOR RADIOPHYSICS AND SPACE RESEARCH

CORNELL UNIVERSITY

ITHACA, NEW YORK 14853

SEMI-ANNUAL STATUS REPORT

NASA Grant NAGW-543

February 15, 1984 - August 15, 1984

ASTEROID LIGHTCURVE INVERSION

Prepared September 1984

Professor Steven J. Ostro
Principal Investigator

TABLE OF CONTENTS

I. INTRODUCTION: Convex-Profile Inversion

The initial six months of research sponsored by NASA Grant NAGW-543 has proceeded rapidly and has yielded a variety of important results. The focus of this research is a new approach, called "convex-profile inversion," to the interpretation of asteroid lightcurves. This technique, developed by the principal investigator in collaboration with R. Connelly, was introduced via the published literature this spring and is already being recognized as the most important contribution since that of H. N. Russell (1906) to solving the problem of extracting information about an asteroid's shape from its lightcurve. Except for the relative handful of objects observable with radar or during stellar occultations, lightcurves provide the only clues to an asteroid's shape. Unfortunately, the form of a lightcurve is influenced by the viewing/illumination geometry and the asteroid's light-scattering behavior, as well as by its shape. Even if we had lightcurves for an asteroid for all physically possible Sun-Earth-asteroid configurations, it would still be impossible to determine the asteroid's shape from disk-integrated measurements. All we can hope to do is to obtain constraints on the shapes of asteroids.

Prior to convex-profile inversion (CPI), almost all efforts to obtain such constraints have invoked an axisymmetric shape described by only one or two parameters. These analyses necessarily discard much of the interesting information that distinguishes individual lightcurves, including all odd harmonics.

CPI obtains a convex profile P from an asteroid's lightcurve. The number of parameters that characterize the profile is limited only

by the number of Fourier harmonics used to represent the parent lightcurve, so our inversion method can preserve much (if not all) of the salient information contained in the parent lightcurve. Whenever four ideal conditions are satisfied, $\underline{P}$ is an estimator for the asteroid's "mean cross section" $\underline{C}$, a convex set defined as the average of all cross sections $\underline{C}(z)$ cut by planes a distance z above the asteroid's equatorial plane. $\underline{C}$ is therefore a 2-D average of the asteroid's 3-D shape. The ideal conditions are: (A) each curve $\underline{C}(z)$ is convex, (B) the asteroid's scattering law is uniform and geometric, (C) the astrocentric declinations δ_S, δ_E of the Sun and Earth are zero and (D) the solar phase angle ϕ is known and nonzero. (CPI's geometrical conventions are such that for any given Sun-Earth-asteroid configuration, the sign of the solar phase angle will correspond to either retrograde or direct rotation.)

To obtain a profile from a lightcurve, we first find the lightcurve's Fourier series: $I(\theta) = \sum \underline{c}_n e^{in\theta}$ and define the radius of curvature function: $r(\theta) = \sum \underline{d}_n e^{in\theta}$, where

$$\underline{d}_n = \underline{c}_n / \underline{v}_n \qquad (1)$$

and $\underline{v}_n$ is a known function (Fig. 1) of the harmonic index n and the solar phase angle ϕ. The profile's cartesian coordinates are

$$\left(-\int_0^\theta r(t) \sin t \, dt, \ \int_0^\theta r(t) \cos t \, dt \right).$$

The profile will be closed and convex only if a set of N linear constraints, $r_i \geq 0$ for $1 \leq i \leq N$, are satisfied. In practice, CPI finds that profile $\underline{P}$ which provides the least-squares estimator for $\underline{C}$ by finding that vector, $\hat{\underline{x}}$, of Fourier coefficients which

satisfies the constraints and is as close as possible to the

vector, $\hat{\underline{x}}$, of the unconstrained Fourier coefficients $\underline{c}_n$.
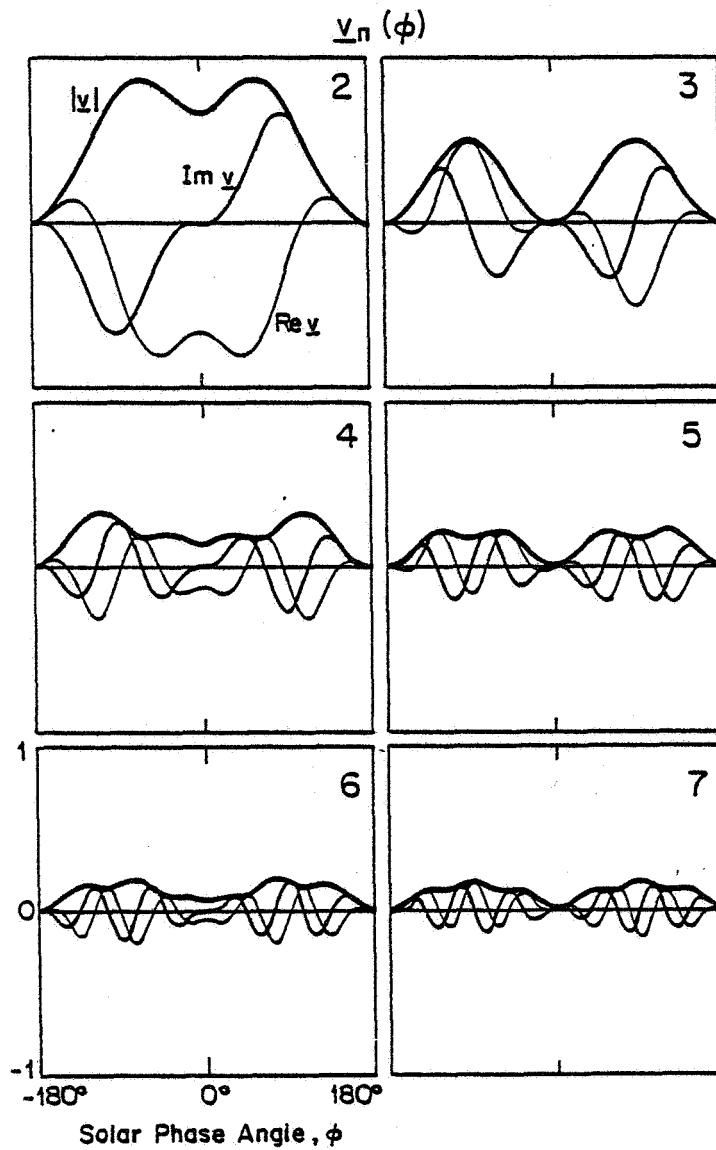
$$\underline{v}_n\,(\phi)$$

FIGURE 1

Figure 2 reproduces figures from Ostro and Connelly (1984)
(i) illustrating CPI's geometric conventions and (ii) showing results
for an asteroid with a D-shaped mean cross section.

Fig. 1. Geometry for two-dimensional asteroid light-curve inversion. The asteroid is a convex profile rotating clockwise, and is shown at rotational phase $\theta = 0°$. The solar phase angle ϕ is indicated, as are the asteroid's illuminated (solid) and unilluminated (dotted) portions. The asteroid's brightness is proportional to the orthogonal projection, in the direction of the Earth, of the visible, illuminated length $I(\theta)$. In the normal-angle parameterization of the profile, the point $P(\theta)$ is on the receding (left-hand) limb and the outward normal $\hat{n}$ at $P(\theta)$ points in the positive x direction when the rotational phase is θ.
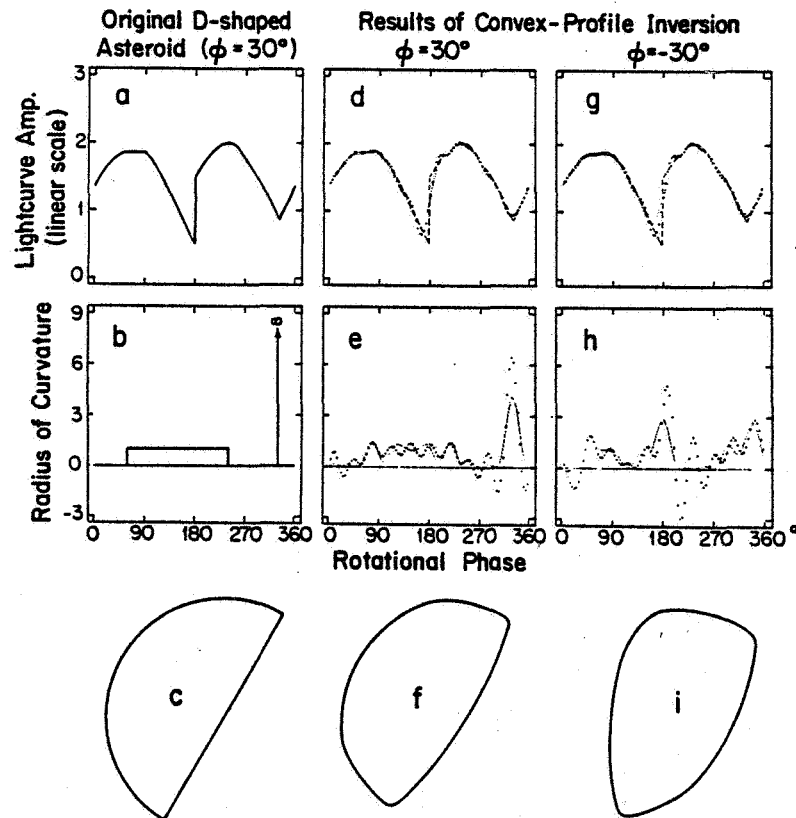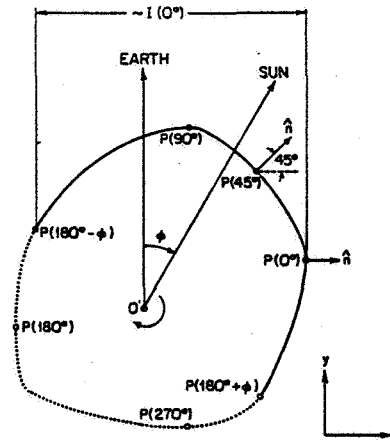

FIG. 3. Convex-profile inversion of the lightcurve obtained at $\phi = 30°$ for a D-shaped, two-dimensional asteroid, $\underline{D}$. Lightcurves, radius-of-curvature functions, and convex profiles are shown in the top, middle, and bottom rows, respectively. The left-hand column shows these quantities for $\underline{D}$. The other columns show results of convex-profile inversion of $\underline{D}$'s lightcurve when $\phi = 30°$ is assumed (middle column) and when $\phi = -30°$ is assumed (right-hand column). The product profile (f) obtained using $\phi = 30°$ differs from $\underline{D}$ because the Fourier representations for the lightcurve and radius-of-curvature function (both of which contain discontinuities) have been truncated to 10 harmonics. (See end of Section II.C.) The severe distortion in the profile (i) obtained using $\phi = -30°$ occurs because the sign of the solar phase angle is wrong. (See Section II.D.) $\underline{D}$'s lightcurve is reproduced as the hand-drawn, dashed curve in (d) and (g) for comparison with the model lightcurves ($\hat{y}$, dots; $\hat{\hat{y}}$, computer-drawn curves) obtained from the unconstrained and constrained Fourier series $\hat{x}$ and $\hat{\hat{x}}$, respectively. In (e) and (h), dots represent $\hat{r}$ and curves represent $\hat{\hat{r}}$. The geometric conventions presented in Fig. 1 are maintained here.

FIGURE 2. Two figures from Ostro and Connelly (1984).

II. SUMMARY OF RESEARCH PROGRESS

The overall objective of the current research is to calibrate and apply CPI. Four tasks were specified in the work plan:

1. Invert high-quality lightcurves.

2. Calibrate CPI's sensitivity to departure from ideal geometric conditions and to lightcurve errors.

3. Explore CPI's sensitivity to non-geometric scattering.

4. Improve CPI's computational efficiency.

As the following summaries demonstrate, progress has been unexpectedly fruitful in elucidating the power and limitations of CPI, in formulating tools for handling profiles as mathematical entities, in suggesting novel uses of the profiles, and in developing new approaches to testing empirical hypotheses about asteroid shapes and scattering properties.
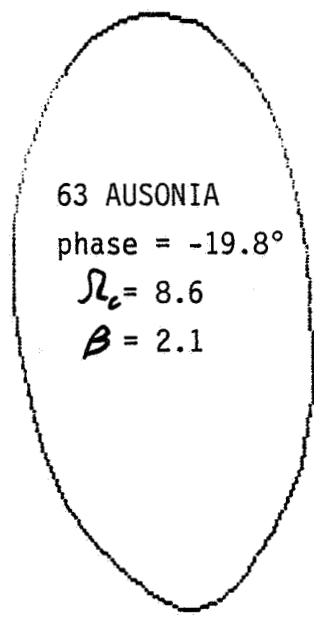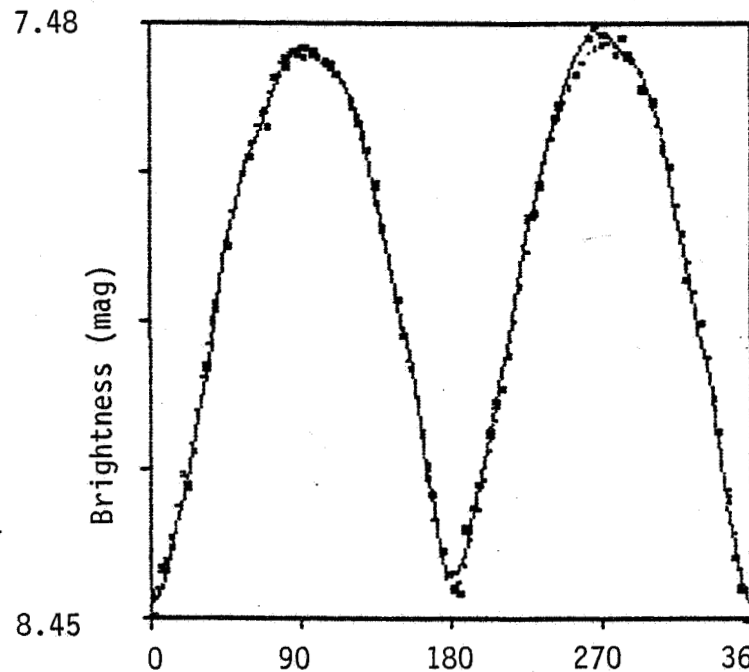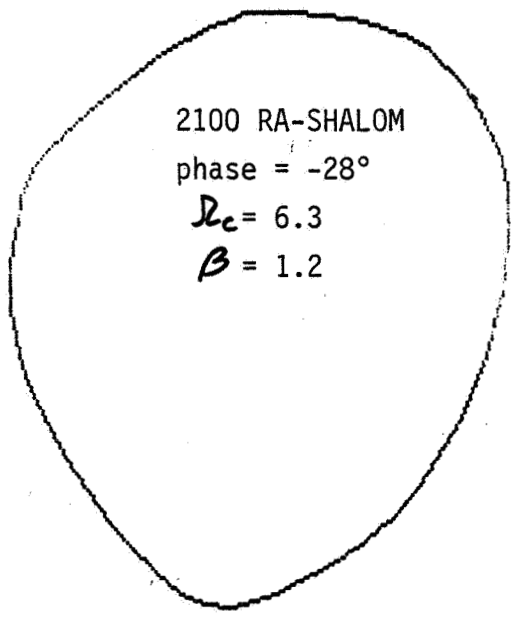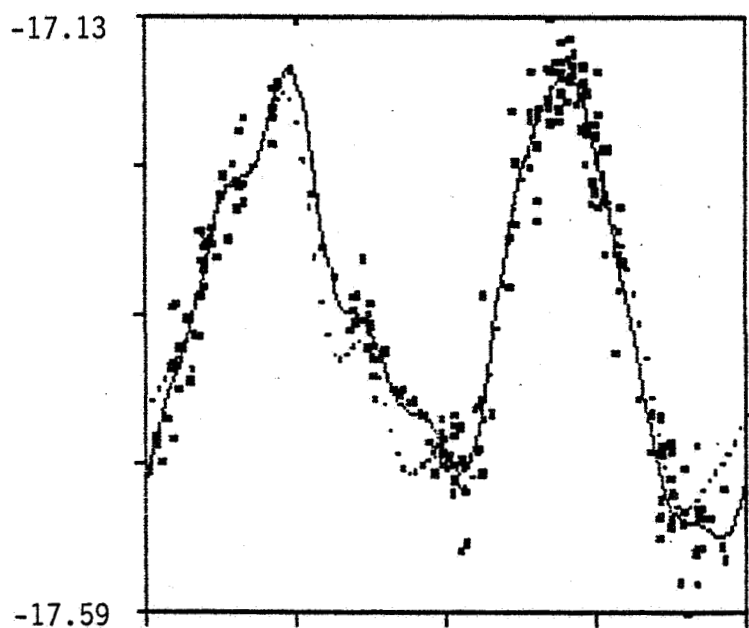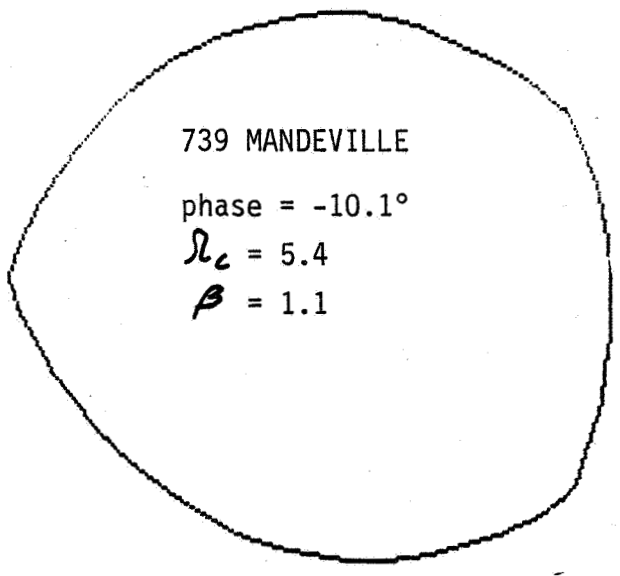
Inversion of Published Lightcurves

The entire asteroid lightcurve literature has been searched and catalogued, and lightcurves for some 50 asteroids have been digitized, inverted, and subjected to various analyses described herein. Because of Eqn. 1, CPI's stability with respect to odd harmonics in $r(\theta)$ deteriorates as $\phi \to 0$ and $v_n \to 0$ for odd n (Fig. 1). A safe rule of thumb seems to be to suppress odd harmonics (hence symmetrizing the profile) when $|\phi| < 10°$. The resulting symmetrized profile P_s is the best available estimator for the asteroid's symmetrized mean cross section C_s. Figure 3 shows CPI output profiles (P or P_s) and lightcurves (y, $\hat{y}$, $\hat{\hat{y}}$) for seven objects. When $|\phi| > 10°$, the chosen
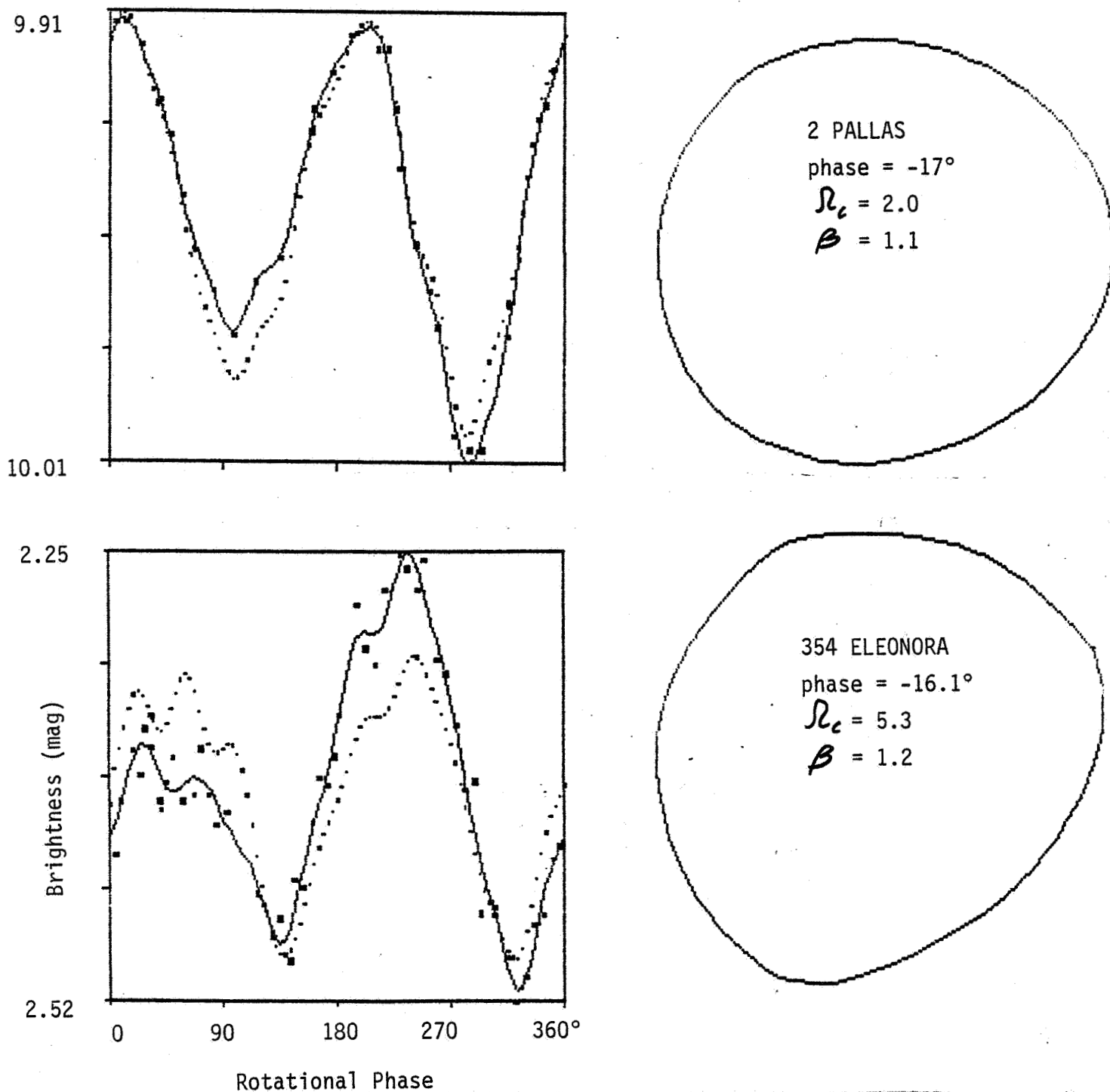
FIGURE 3. Convex profiles for seven asteroids. In the lightcurve plots, large, rectangular symbols are the data y, the solid curve is the unconstrained model $\hat{y}$, and the dotted curve is the constrained model $\hat{\hat{y}}$ corresponding to the profile. Sources of the lightcurves are: Pallas, Binzel (1984) in prep.; Eleonora, Zappalà and van Houten-Groenveld (1979), A. A. Supp. 35, 220, Fig. 19; Mandeville, Zappalà et al. (1983), Icarus 56, 325, Fig. 28; Ra-Shalom, Ostro et al. (1984), Icarus 60, in press; Ausonia, Lagerkvist (1981), A. A. Supp. 44, 401, Fig. 3; Roxane, Lagerkvist et al. (1982), Sun and Planetary System (Fricke and Teleki, eds.), p. 209; Hektor, Dunlap et al. (1969), Astron. J. 74, 796, Fig. 8.

739 MANDEVILLE

phase = -10.1°

Ω_c = 5.4

β = 1.1

2100 RA-SHALOM

phase = -28°

Ω_c = 6.3

β = 1.2

63 AUSONIA

phase = -19.8°

Ω_c = 8.6

β = 2.1

Brightness (mag)

Rotational Phase

317 ROXANE

SYMMETRIZED

phase = 4°

624 HEKTOR

SYMMETRIZED

phase = 4°

Brightness (mag)

11.89

12.55

0.00

1.85

0   90   180   270   360°
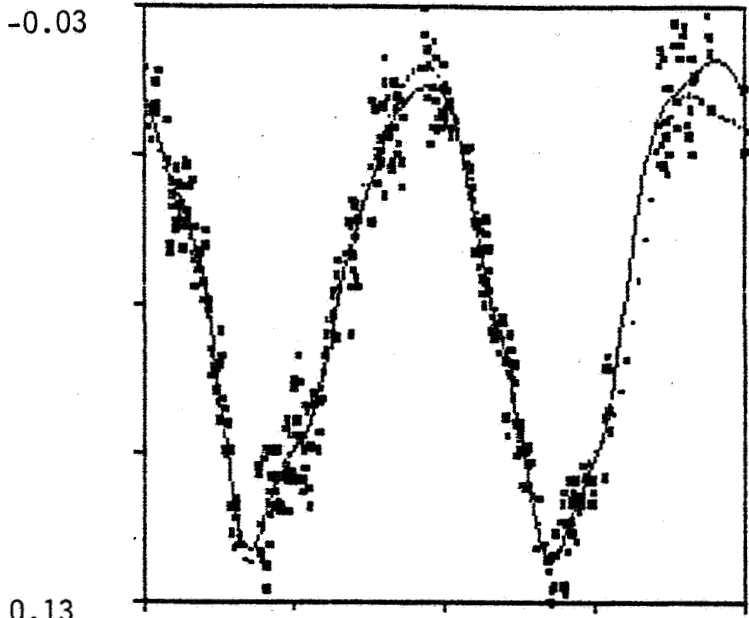
Rotational Phase
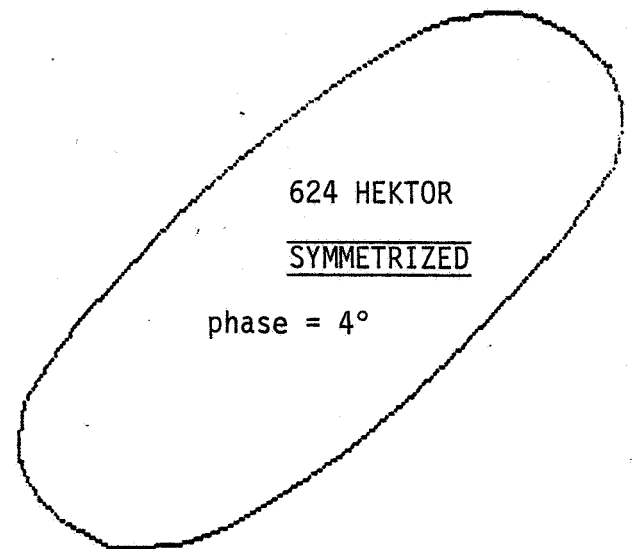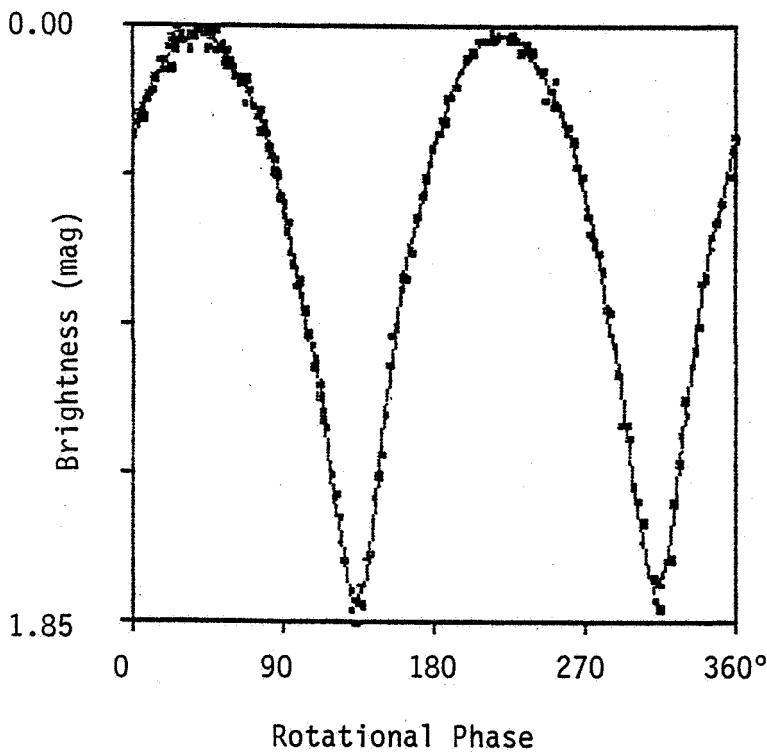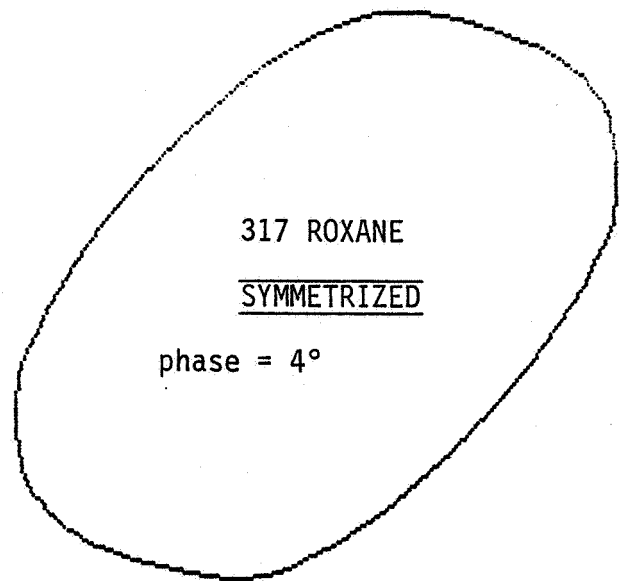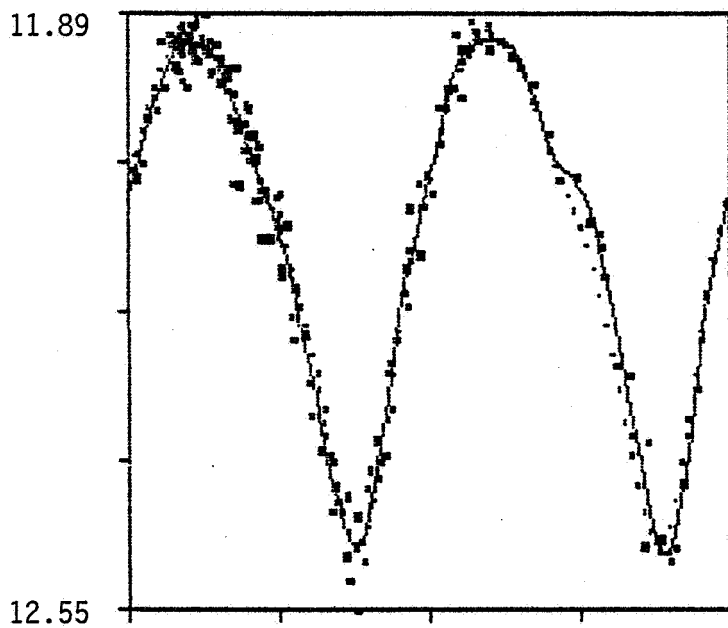
sign of ϕ corresponds to direct rotation and a southerly view of the asteroid.

Computational Efficiency

The most time-consuming operation in CPI involves finding that Fourier vector $\hat{\underline{x}}$ for the lightcurve which satisfies the constraints, $r_i \geq 0$, i = 1 to N, and is closest to the unconstrained vector $\hat{\underline{x}}$. Our solution of this "quadratic programming problem" uses a straightforward, but somewhat inefficient, recursive projection algorithm.

Lengthy experimentation with various modifications to our algorithm suggest that the most economically sound approach is simply to pre-order the N constraints from the most negative r_i to the most positive r_i. This yields "convexification" times between 20% and 50% of those experienced without the heuristic.

Lightcurves of Geometrically-Scattering Ellipsoids (GSE's)

In efforts to test CPI by inverting lightcurves of known shape and scattering law, we realized that whereas it was known that lightcurves of GSE's could be generated analytically, a simple formula for such lightcurves was unavailable. We derived such a formula and discovered properties of GSE lightcurves that let us test the hypothesis that a given asteroid lightcurve could be due to a GSE. Principal results are:

1. Given the equation $(\underline{x}^T \underline{Q} \underline{x} = 1)$ for an a×b×c GSE and directions $\hat{\underline{s}}$ and $\hat{\underline{e}}$ of the Sun and Earth, the lightcurve has the form:

$$I = \pi abc[(\underline{e}^T Q \underline{e})^{1/2}(\underline{s}^T Q \underline{s})^{1/2} + \underline{e}^T Q \underline{s}]/2(\underline{s}^T Q \underline{s})^{1/2}$$

2. At opposition ($\hat{\underline{e}} = \hat{\underline{s}}$), I^2 has harmonics 0 and 2 only.

3. The fractional error incurred using an opposition lightcurve I_0 to approximate a non-opposition lightcurve I satisfies:

$$(I_0 - I)/I \le \varepsilon \equiv \rho^2 \tan^2(\phi/2)$$

where ϕ is the solar phase angle and $\rho = a/c$ is the ratio of the longest axis to the shortest. Figure 4 plots ε vs. ϕ for several values of ρ. For $\rho \le 4$, the error is less than 1% if ϕ is only a few degrees, but is of order 10% for $\phi \sim 20°$.

4. The contribution to I of harmonics other than 0 and 2 depends on ρ and ϕ. For any lightcurve, we can calculate a statistic $\hat{\tau}$, and then use $\hat{\tau}$ to find the minimum value of ρ that permits the hypothesis that "the lightcurve can be due to a GSE" to stand. The minimum value of ρ is:

$$\rho_{min} = [(1 + \hat{\tau}^{1/2})^{1/2} - 1]^{1/2}/\tan(\phi/2)$$

where

$$\hat{\tau} = \frac{\sum\limits_{\substack{n \neq 0,2}}^{M} (a_n^2 + b_n^2)}{2a_0^2 + \sum\limits_{n=1}^{M} (a_n^2 + b_n^2)} \le \tau \equiv (2\varepsilon + e^2)^2$$

where a_n and b_n are the Fourier cosine and sine coefficients in the M-harmonic series for I^2. Figure 5 plots curves of ρ_{min} vs. τ for several values of ϕ. Positions of asteroid numbers denote minimum values of a/c required to forestall rejection of the hypothesis that the asteroid is a GSE.
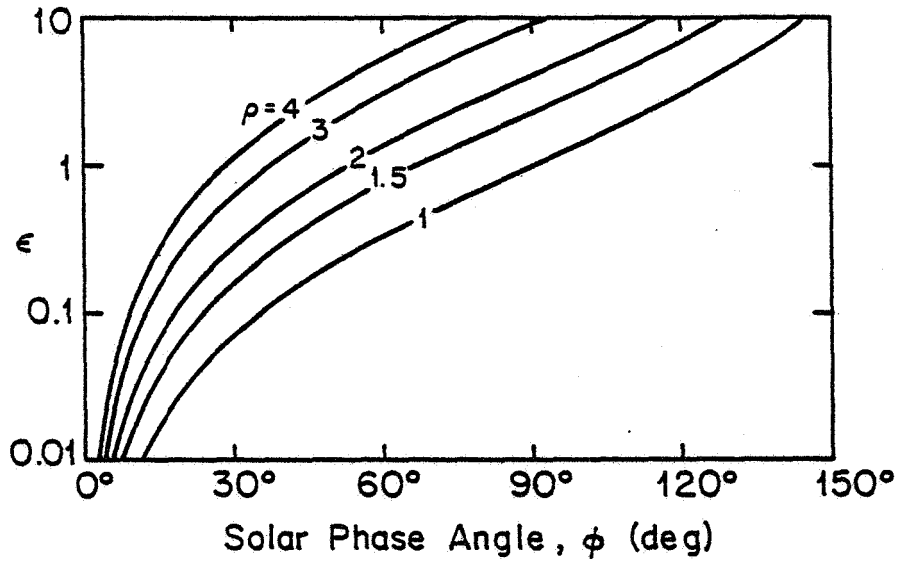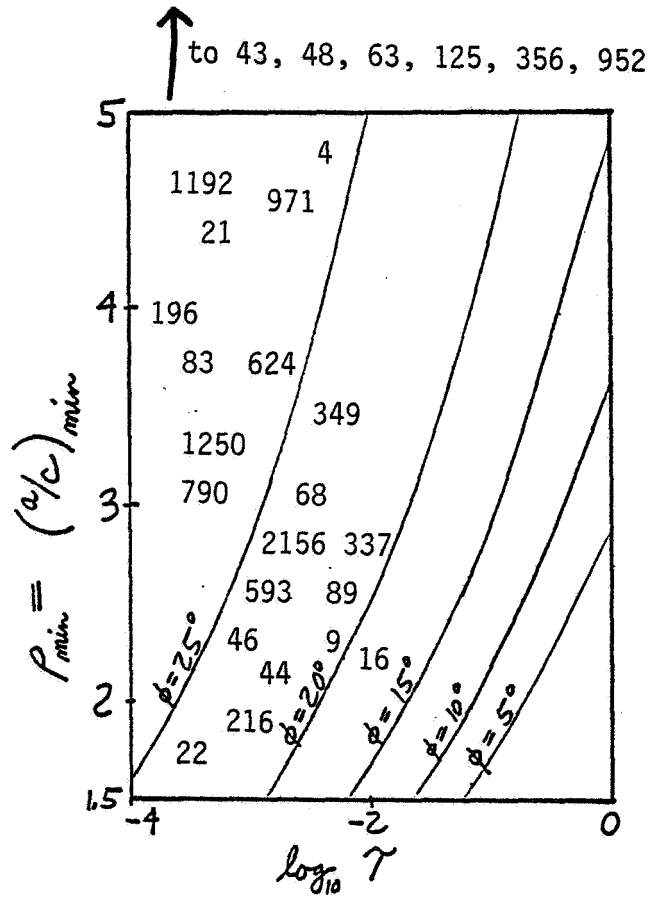
FIGURE 4

FIGURE 5

Sensitivity of CPI to Viewing/Illumination Geometry

How reliable is $\underline{P}$ as an estimator for $\underline{C}$ when Condition C (astrocentric declinations δ_E and δ_S of the Earth and the Sun are zero) is violated? For any given object, the answer to this question depends on δ_E, δ_S, and ϕ. To explore this particular type of systematic effect, we have generated and inverted lightcurves of GSE's for non-ideal geometries and various values of b/a and c/a which sample the parameter space: $10° \leq \phi \leq 80°$, b/a = 0.2 and 0.4, and $0.05 < c/a < b/a$.

For any given ellipsoid and solar phase angle, the field of possible viewing/illumination geometries is conveniently displayed in a plot (Fig. 6) of δ_S vs. ($\delta_E - \delta_S$). Figure 6 shows three of our several dozen "geometric distortion" plots, selected to illustrate a few 2-D cuts through the 5-D space. A major conclusion is that if $\left|\delta_E\right|$, $\left|\delta_S\right| > \left|\phi\right|$, then distortion is minimal when δ_E is between $\left|\phi\right|$ and $-\delta_S$ (i.e., when $\hat{e}$ and $\hat{s}$ are on opposite sides of the equatorial plane) and is most severe when δ_S is between $\left|\phi\right|$ and δ_E (i.e., when $\hat{s}$ is between $\hat{e}$ and the equatorial plane).

Quantitative Comparison of Profiles

Recognizing the desirability of quantifying the relationship between profiles rather than merely making verbal statements of subjective impressions, the principal investigator surveyed approaches to this type of problem within the pattern-recognition literature. It seems appropriate to define the distance Ω between any two profiles $\underline{P_1}$ and $\underline{P_2}$ as
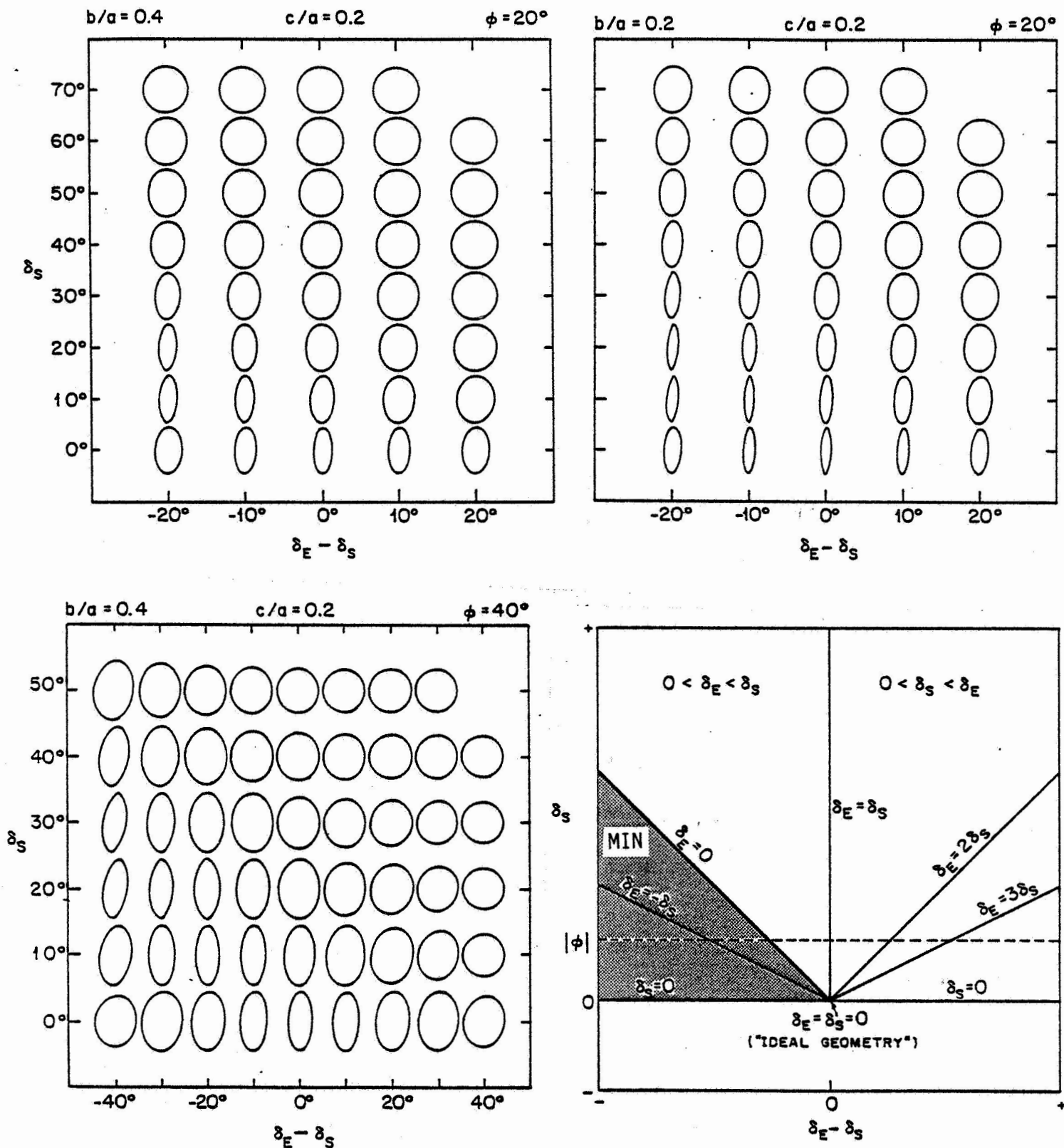
FIGURE 6. "Geometric distortion plots." Application of CPI to GSE lightcurves obtained when Condition C (= = 0) is violated yields profiles that deviate from the ellipsoid's mean cross section (C, at the origin of each array of profiles). The three arrays illustrate distortion for three sets of values of b/a, c/a, and φ. The bottom right figure shows some contours of constant δ_E or constant δ_S . Note that the Earth is north of the equator except within the stippled area. Distortion is minimal within the region "MIN."

$$\Omega = 10 \min_{\theta_{rot}} \left| \underline{d}_1/d_{10} - \underline{d}_2 e^{j\theta_{rot}}/d_{20} \right|$$

where $\underline{d}_i$ is the vector of complex Fourier coefficients in the expansion of P_i's radius-of-curvature function and d_{i0} is the constant, or zero-harmonic term, in that expansion. This distance measure is rotation- and scale-invariant and defines a Euclidean metric.

Measures of Noncircularity and Elongation

We define (i) the "noncircularity" Ω_c as the distance between a given profile and a circle, and the "maximum breadth ratio" β as the ratio of a profile's maximum breadth to its minimum breadth. These statistics incorporate all the information in a parent lightcurve, and are now being calculated for all our asteroid profiles.

In the past, the lightcurve amplitude Δm has been used as a measure of an asteroid's noncircularity and elongation. This approach would be justified if every asteroid were a geometrically scattering ellipsoid and every lightcurve were obtained at zero solar phase angle and under equatorial geometry. For the purpose of using actual lightcurves to compare the shapes of real asteroids, the statistics Ω_c and β are a priori preferable to Δm and also permit a distinction between noncircularity and elongation. As a case in point, compare the pairs of values of Δm, Ω_c, and β for two lightcurves of 15 Eunomia at different solar phase angles (Fig. 7), and note values of Ω_c and β for the profiles in Fig. 3.
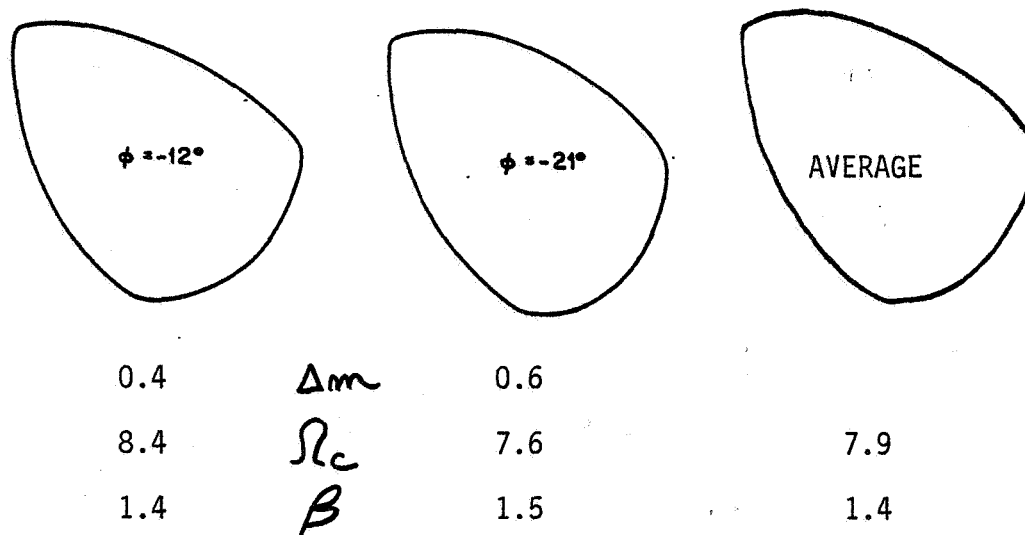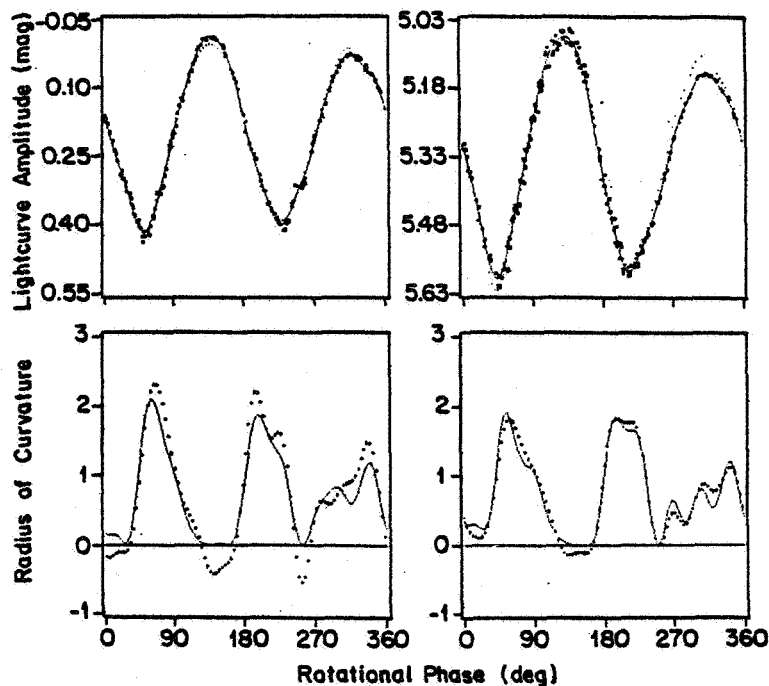
FIG. 7. Convex profiles for asteroid 15 Eunomia. Lightcurves obtained at solar phase angles $\phi = -12°$ (Fig. 8 of Groeneveld and Kuiper, 1954) and $\phi = -21°$ (Fig. 14 of van Houten-Groeneveld and van Houten, 1958) were digitized and inverted as described in the text. The signs for ϕ correspond to retrograde rotation, as deduced by the cited authors. (See Section II.D.) In each of the top figures, the large rectangular symbols are the lightcurve data y, the solid curve represents the lightcurve $\hat{y}$ derived from the unconstrained Fourier fit and the tiny dots represent the lightcurve $\hat{y}$ derived from the constrained fit, i.e., from the convex-profile inversion. In the middle figures, the radius-of-curvature functions $\hat{r}$ and $\tilde{r}$ are represented by symbols and solid curves, respectively. The profiles are shown at rotational phase $\theta = 0°$, and the geometrical conventions given in Fig. 1 are maintained here. Hence, at secondary lightcurve maximum ($\theta \sim 320°$), each profile would be rotated clockwise $\sim320°$ and the uppermost side would face toward Earth (i.e., toward the top of the page). The relation between the rotational phases of the two profiles (and of the corresponding lightcurves and radius-of-curvature functions) was chosen to maximize the cross-correlation between $\hat{r}(\theta)$ for $\phi = -12°$ and $\hat{r}(\theta)$ for $\phi = -21°$. (This approach might prove useful in refining estimates of asteroid rotation periods.) In these and all other inversions presented in this paper, each Fourier series was truncated to $M = 10$ harmonics and the inequality constraints (8) were enforced at $N = 96$ equally spaced values of θ.

FIGURE 7. Lightcurve amplitude Δm, noncircularity Ω_c, and maximum breadth ratio β for two independent lightcurves of 15 Eunomia have been added to this reproduction of Fig. 7 from Ostro and Connelly (1984). Note also the average of the two profiles, and its values of Ω_c and β.

Algebraic Manipulation of Profiles

To the extent that ideal conditions are satisfied, profiles obtained for different solar phase angles should be similar. In different words, they should not be "far apart" because each is an estimator for the asteroid's (unique) mean cross section. Therefore it makes sense to obtain appropriately weighted averages of independent profiles. In practice, this is most easily done by manipulating the Fourier vectors d_i for $r_i(\theta)$ corresponding to the P_i. Thus, CPI is able to combine the information contained in any number of independent lightcurves to yield a 2-D average of an asteroid's 3-D shape. Figure 7 shows the average of two Eunomia profiles.

Sensitivity of CPI to Non-Geometric Scattering and Non-Convexity

Efforts are underway to calibrate the distortion introduced into a profile P as an estimator for the mean cross section C when ideal conditions A (convexity) and B (geometric scattering) are violated. J. Lambert (Univ. of New Mexico) has used a numerical integration routine to generate lightcurves of ellipsoids having non-geometric scattering laws, for various geometries. His lightcurves, which include a few "standard" GSE's, are being inverted at Cornell. First results indicate that limb darkening results in a profile that is more elongated than the parent ellipsoid's mean cross section. In other words, P is "less circular" than C. In contrast, departure from ideal viewing/illumination geometry (Condition C) frequently causes P to be more circular than C (Fig. 6). Perhaps these two systematic effects offset each other. In any event, given adequate prior knowledge of

viewing/illumination geometry or scattering law, we can try to correct $\underline{P}$ for non-ideal conditions via ad hoc addition or subtraction of some fraction of a circle.

In a different experiment, M. A. Barucci (Instituto de Astrofisica Spaziale, Consiglio Nazionale delle Ricerche, Rome) has generated laboratory lightcurves of a stone fragment for a variety of viewing/illumination geometries. The lightcurves have been inverted at Cornell, and photographs of the fragment have been requested from Barucci to provide a "ground truth" fiducial for calibration of CPI.

Propagation of Lightcurve Noise into Profile Error

The previous paragraphs have focused on systematic sources of error in $\underline{P}$, i.e., on distortion in $\underline{P}$ caused by departure from ideal conditions. Since actual lightcurves are contaminated with measurement errors, any profile obtained via CPI may be corrupted accordingly, and it is necessary to examine the nature of this error propagation.

Whereas actual lightcurve measurement errors may arise from systematic sources (e.g., sky-background removal, intermittent cirrus, imperfect color matches between asteroid and comparison star, etc.) as well as from photon-counting stochastic errors, one can always compute an "effective" standard deviation in the overall noise due to all sources. As this standard deviation becomes an increasingly large fraction of the lightcurve amplitude, $\underline{P}$ will become increasingly distorted. The distortion will be magnified if the lightcurve contains big gaps or is sampled at an insufficient rate.

We have investigated the three effects of noise, gaps, and undersampling, acting alone and in concert, on profiles obtained from lightcurves of GSE's and the D-shaped object in Fig. 2. Propagation of statistical error is being modeled by using a random number generator to produce Gaussian noise samples, scaling the standard deviation to some fraction of the lightcurve amplitude, adding the noise to the lightcurve, and doing the inversion. This entire process is repeated to build up a family of realizations of the random process in the form of a set of profiles, P_i. The distortion in the P_i is evident visually and can be quantified by the distances of the P_i from C. Figure 8 illustrates some results of five-profile simulations on GSE lightcurves. (Distortion is worse for the D-shaped object.)

At this point, an appropriate guideline seems to be that lightcurves targeted for CPI should be sampled at intervals no larger than 5° and should have noise levels $\lesssim$ 3% of the lightcurve amplitude. Since CPI's ideal conditions on viewing/illumination geometry, etc., will rarely be satisfied exactly, it clearly is vital that the lightcurve data be of high quality.

Current error-propagation work is focusing on actual asteroid lightcurves, with the objective of placing formal errors on Ω_c and β as well as on the profiles themselves.

FIGURE 8. Error propagation into profiles obtained from lightcurves of a GSE with b/a = 0.4, c/a = 0.2, and $\delta_E = \delta_S = 0$. Sets of five simulation profiles are labeled with the sampling interval in degrees, the noise level (expressed as a percentage of the lightcurve amplitude), and the distance Ω from the parent ellipsoid's mean cross section. "INTER-EX OUT" denotes deletion of four, 40° inter-extremum sections of data, and "MIN OUT" denotes deletion of a 40° section of data centered on one minimum.
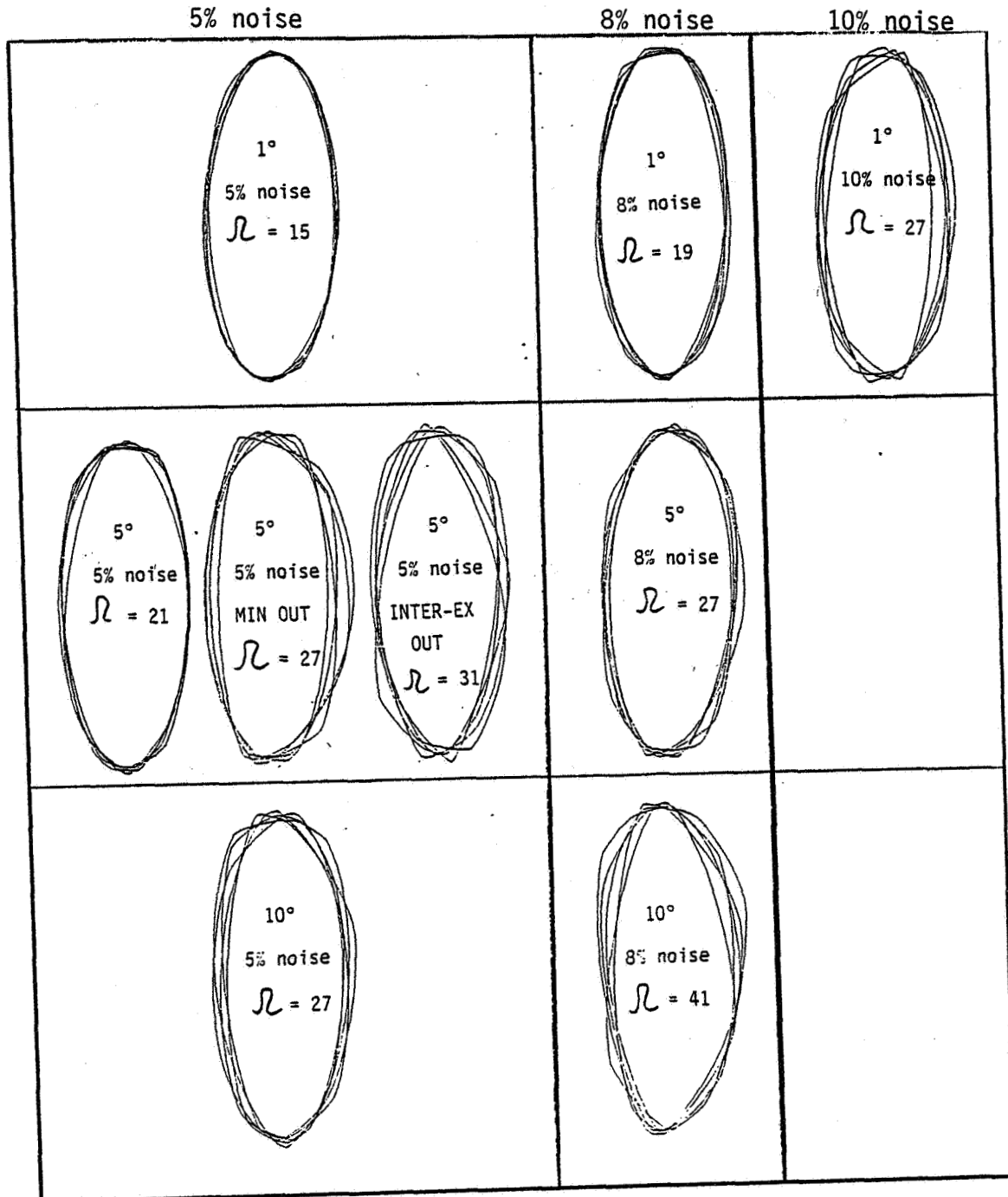
III. FUNDING STATUS

Spending during the current report period was at the anticipated rate. A graduate student in Applied and Engineering Physics, Mark Dorogi, was hired full time over the summer as a research assistant. A Physics senior, Anthony Ferro, will be employed as a part-time programmer this fall.

IV. PUBLICATION OF RESULTS

The following papers report results of the research supported under NAGW-543:

1. Convex Profiles from Asteroid Lightcurves, S. J. Ostro and R. Connelly, Icarus 57, 443-463 (1984).

2. Ellipsoids and Lightcurves, R. Connelly and S. J. Ostro, Geometriae Dedicata, in press (1984).

A paper (abstract appended) reporting some of the more recent results has been submitted to the 1984 Meeting of the Division for Planetary Sciences of the American Astronomical Society.

Additionally, the principal investigator has given seminars on CPI at the Arecibo Observatory, the Planetary Science Institute (Tucson), the Jet Propulsion Laboratory, and Cornell.

Abstract of paper submitted to the 16th Annual Meeting of the Division for Planetary Sciences of the American Astronomical Society:

Convex-Profile Inversion of Asteroid Lightcurves: Calibration and Application of the Method

S. J. Ostro, M. D. Dorogi, and R. Connelly (Cornell)

Convex-profile inversion (Ostro and Connelly, 1984, Icarus 57, 443) is a method for obtaining a convex profile, P, from asteroid lightcurve data. Whenever four ideal conditions are satisfied, P is an estimator for the asteroid's "mean cross section" C, a convex set defined as the average of all cross sections $C(z)$ cut by planes a distance z above the asteroid's equatorial plane. C is therefore a 2-D average of the asteroid's 3-D shape. The ideal conditions are: (A) each curve $C(z)$ is convex, (B) the asteroid's scattering law is uniform and geometric, (C) the astrocentric declinations δ_S, δ_E of the Sun and Earth are zero, and (D) the solar phase angle $\phi \neq 0$. The method has been tested by inverting lightcurves generated analytically for geometrically scattering ellipsoids (GSE's) with semiaxes $a \geq b \geq c$. Using a suitably defined "distance measure" to quantify the difference between any two profiles, we have calibrated the deviation of P from C for GSE's as a function of lightcurve noise level, rotation-phase sampling interval $\Delta\theta$, and departure from ideal conditions. The coupling between these factors is considerable. If the rms noise due to all sources is ~ 3% of the lightcurve's peak-to-valley amplitude, then $P \approx C$ if $\Delta\theta < 5°$. If $|\delta_E|$, $|\delta_S| > |\phi|$, then distortion of P is minimal when δ_E is between 0 and $-\delta_S$ but severe when δ_S is between 0 and δ_E. We currently are calculating P for high-quality, published lightcurves. The "distance" between P and a circle provides a gauge of the asteroid's nonsphericity and (in contrast to the lightcurve amplitude) incorporates all the information contained in the lightcurve.